Reversible Local and Global Switching in Multicomponent Supramolecular Networks: Controlled Guest Release and Capture at the Solution/Solid Interface

Shern-Long Lee,[*,†,⊥] Yuan Fang,[†] Gangamallaiah Velpula,[†] Fernando P. Cometto,[‡,§] Magalí Lingenfelder,[‡,§] Klaus Müllen,[∥] Kunal S. Mali,[*,†] and Steven De Feyter[*,†]

[†]Division of Molecular Imaging and Photonics, Department of Chemistry, KU Leuven-University of Leuven, Celestijnenlaan 200F, B-3001 Leuven, Belgium, [‡]Max Planck-EPFL Laboratory for Molecular Nanoscience, and [§]Institut de Physique de la Matière Condensée, Ecole Polytechnique Fédérale de Lausanne, CH 1015 Lausanne, Switzerland, and [∥]Max Planck Institute for Polymer Research, D-55128 Mainz, Germany [⊥]Present address: Department of Chemistry, National Taiwan University, Taipei, Taiwan 10617.

ABSTRACT Dynamically switchable supramolecular systems offer exciting possibilities in building smart surfaces, the structure and thus the function of which can be controlled by using external stimuli. Here we demonstrate an elegant approach where the guest binding ability of a supramolecular surface can be controlled by inducing structural transitions in it. A physisorbed self-assembled network of a simple hydrogen bonding building block is used as a switching platform. We illustrate that the reversible transition between porous and nonporous networks can be accomplished using an electric field or applying a thermal stimulus. These transitions are used to achieve controlled guest release or capture at the solution–solid interface. The electric field and the temperature-mediated methods of guest release are operative at different length scales. While the former triggers the transition and thus guest release at the nanometer scale, the latter is effective over a much larger scale. The flexibility associated with physisorbed self-assembled networks renders this approach an attractive alternative to conventional switchable systems.

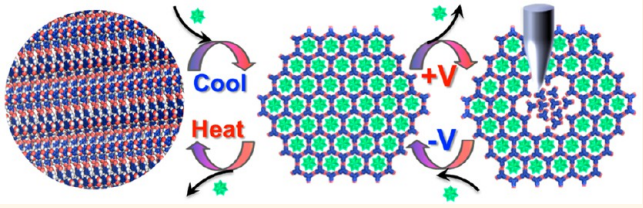

KEYWORDS: stimuli-responsive systems · controlled guest release · self-assembly · scanning tunneling microscopy · liquid–solid interface

Surfaces that respond to external stimuli in a well-defined manner are crucial in the development of functional supramolecular systems. As a consequence, stimuli-responsive behavior of molecular materials on surfaces has become an integral part of design concepts in material science and supramolecular chemistry. This theme of research is largely inspired by efficient biomolecular processes such as protein assemblies operating at dynamic interfaces like cell membranes. The past decade has witnessed significantly increased research activity in the field of smart surfaces, where the fundamental objective is to induce reversible structural changes in supramolecular surfaces by application of an external trigger with an intent to achieve reversible changes in function. The combined efforts of the molecular synthesis, supramolecular chemistry, and surface science community have led to exciting opportunities in the development of dynamic, reversibly switchable surfaces with potential applications in molecular switches and motors, biological sensors, tunable filtration membranes, and drug delivery vehicles.[1−4]

Chemisorbed self-assembled monolayers (SAMs), bilayers, polymers, and semiconductor metal oxide thin films have been employed as active components in the design of switchable surfaces. For organic surfaces, the molecular or macromolecular entities are covalently attached onto a solid

* Address correspondence to sllee@ntu.edu.tw, kunal.mali@chem.kuleuven.be, steven.defeyter@chem.kuleuven.be.

Received for review September 27, 2015 and accepted October 29, 2015.

Published online November 09, 2015
10.1021/acsnano.5b06081

surface, and their response to external stimuli, such as light, heat, pH, surface potential, *etc.*, is examined. Light-driven photochromism of azobenzene units, for example, is a spectacular strategy that involves reversible photoisomerization leading to changes in surface properties.[5,6] A valuable approach in this context is the use of low-density ionizable alkanethiol monolayers, which allow conformational transitions using electric potential.[7] A critical bottleneck, however, is the complexity involved in the design of low-density monolayers with sufficient space between chemisorbed molecules, allowing efficient conformational transition.[8]

Physisorbed monolayers of organic molecules provide a convenient alternative to chemisorbed systems in two aspects. Since the intermolecular and interfacial interactions are relatively weak, dynamic reconstitution of noncovalent bonds involved in the assembly process is possible so that better control over structure formation as well as reversible switching becomes possible.[9,10] Second, the density of physisorbed networks can be readily manipulated by simply changing the concentration of building blocks in solution.[11,12] Similar to the switchable systems listed above, reversible transitions in physisorbed single molecules as well as self-assembled monolayers have been studied both under ultrahigh vacuum (UHV) conditions and at the more practical solution−solid interface. Switching between different states has been achieved by using additives,[13−16] temperature,[17−20] light,[21−24] pH,[25] surface potential,[26,27] electric field,[28−32] as well as ion triggers.[33,34] A large number of switchable physisorbed monolayers studied so far involved a single component adsorbed onto the solid surface, while reversible switching in multicomponent supramolecular networks has been rarely studied.[21,22,31]

In this contribution, we demonstrate a unique combination of a switchable surface with host−guest chemistry. A low-density supramolecular network made up of 1,3,5-tris(4-carboxyphenyl)benzene (BTB, Scheme 1) is used as a switchable platform in a scanning tunneling microscopy (STM) setup. Here, STM acts both as a visualization and as a nanomanipulation tool. The transition from the low- to the high-density network (and *vice versa*) of BTB can be accomplished using an electric field applied between the STM tip and the substrate.[35] The compression and expansion of the host network is used to "squeeze" out and reaccommodate the guest molecules, respectively, thereby enabling their controlled release and capture at the solution−solid interface. We demonstrate that the two-component host−guest systems involving this switchable platform can be reversibly interchanged locally at the nanometer scale using an electric field and also globally using a thermal stimulus. Most importantly, the local and global methods of switching introduced here represent complementary approaches of guest release. This strategy not only enriches the realm of switchable systems but also opens up potential applications in controlled guest release.

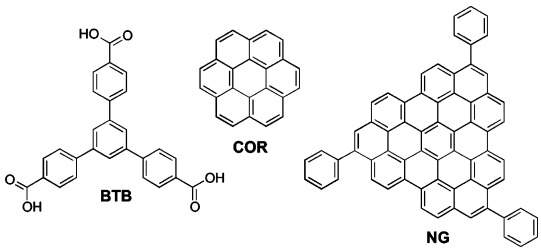

Scheme 1. Molecular structures of 1,3,5-tris(4-carboxyphenyl)-benzene (BTB), coronene (COR), and nanographene (NG).

RESULTS AND DISCUSSION

Scheme 1 shows the chemical structures of molecules used in this study. BTB forms the host network, whereas COR and NG are used as guest species. Figure 1 summarizes the electric-field-induced reversible transition between low-density (open) and compact (closed) structures of BTB realized at the 1-octanoic acid/highly oriented pyrolytic graphite (HOPG) interface. Six $R^2_2(8)$ dimers exist per hexagon in the honeycomb structure, whereas possibly no $R^2_2(8)$ dimer exists in the compact structure. This assembly may be sustained by weak aromatic C−H···O═ interactions. BTB is known to show rich assembly behavior when adsorbed at the organic solution/HOPG interface. At relatively higher concentrations, it is known to form up to three types of densely packed networks, whereas lower concentrations yield a low-density porous structure.[18,36] The low-density porous network has been found to be stable in a number of solvents ranging from different alkanoic acids to relatively nonpolar solvents such as 1-phenyloctane and dodecane.[37] It must be noted that the compact structure presented in Figure 1b is only accessible at positive values of substrate bias. The STM image provided in Figure 1c demonstrates the ease of structural transition between the densely packed and open porous network of BTB by simply switching the polarity of the voltage applied to the substrate. The transition is fast and fully reversible. The reversibility does not depend on the history of the applied bias (*i.e.*, the initial substrate bias).[31] Cometto *et al.* have proposed a conformation-dependent charge transfer mechanism to explain the phase transitions observed in BTB networks.[35] Their experimental results demonstrate that, barring the voltage window between −0.35 and +0.40 V, the BTB networks could be switched between the two states by changing the polarity of the sample bias within the experimentally sampled voltage range of −1.0 to +1.0 V.

COR[38] and NG[39] were chosen as model guest systems as they have been successfully used in host−guest experiments in the past. While COR does not form a stable self-assembled monolayer without a host

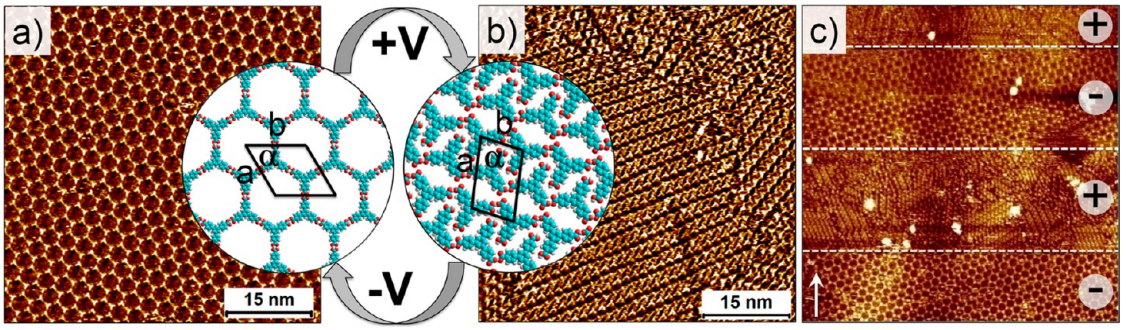

Figure 1. Substrate-bias-induced structural transition in the monolayers of BTB at the 1-octanoic acid/HOPG interface. (a) Low-density structure of BTB formed at negative substrate bias. The unit cell parameters are $a = 3.2 \pm 0.2$ nm, $b = 3.1 \pm 0.2$ nm, $\alpha = 59 \pm 2°$. (b) Compact structure of BTB obtained at positive substrate bias. The unit cell parameters are $a = 2.5 \pm 0.3$ nm, $b = 1.6 \pm 0.2$ nm, $\alpha = 78 \pm 3°$. Molecular models depicting the transition between the two structures are superimposed on the STM images. (c) STM image showing the ease of structural transition upon switching the polarity of substrate bias within a single scan. ([BTB] = 10% from a saturated solution). The white arrow in panel (c) indicates the scan direction. Imaging conditions: $V_{bias} = \pm 900$ mV, $I_{set} = 100$ pA.

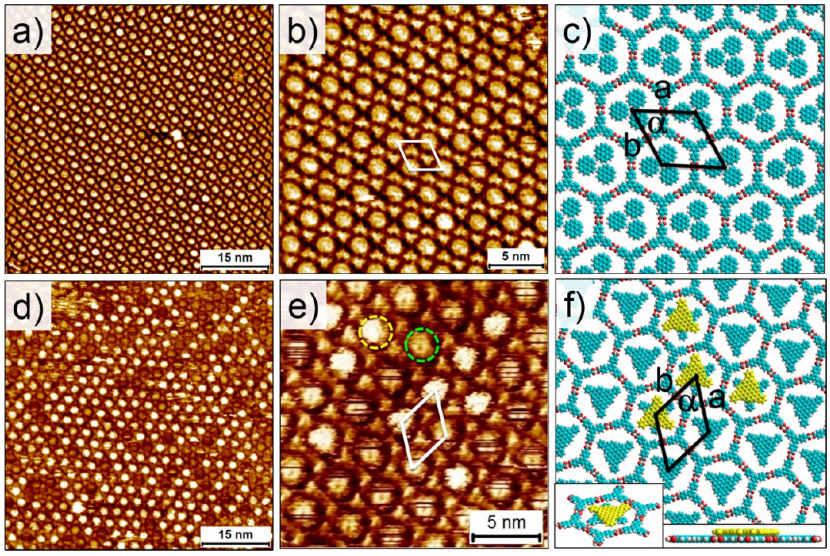

Figure 2. Host–guest systems based on the low-density open structure of BTB at the 1-octanoic acid/HOPG interface. (a,b) Large- and small-scale STM images of the BTB–COR host–guest system, respectively. (c) Molecular model depicting the plausible host–guest structure formed on the surface. (d,e) Large- and small-scale STM images of the BTB–NG host–guest system, respectively. The green and yellow circles indicate single and stacked NG molecules in the pore, respectively. (f) Molecular model depicting the BTB–NG network. The stacked structures are represented by an additional NG molecule (yellow) in the pore. The insets in the molecular model show the tilted and side view of the stacked NG molecules. Imaging conditions: $V_{bias} = -800$ mV, $I_{set} = 100$ pA (also see Figure S4 in the Supporting Information).

network at the solution–HOPG interface, NG gives rise to an extended network that is stable to STM scanning at room temperature. The NG network, however, does not reveal a dependence on the polarity of the substrate bias (Figure S1 in the Supporting Information). Panels (a) and (b) in Figure 2 provide large- and small-scale STM images of the BTB–COR host–guest system, respectively. The cavities of the BTB network appear bright, indicating COR adsorption. No individual guest molecules could be resolved, possibly in view of their lateral mobility in the BTB cavities. Eder *et al.* have proposed the presence of three coronene molecules per BTB cavity based on molecular dynamics (MD) simulations (Figure 2c).[38]

For the BTB–NG system, however, capture of only one NG molecule per BTB cavity is anticipated based on the size of the host cavity (~2.8 nm) and the guest (~2.1 nm). Due to the disparity in the size and shape of the BTB cavity and NG, the NG molecules can rotate in the cavity. This is indicated by the appearance of NG in STM images, where they appear disc-like instead of triangular in shape. Another peculiar feature of the BTB–NG system is the variation in the STM contrast of NG guests as evident from STM images provided in Figure 2d,e. Some NG guests appear brighter than others, and we ascribe these bright features to π-stacked dimers of NG (Figure 2f and Figure S2 in the Supporting Information). The tendency to form

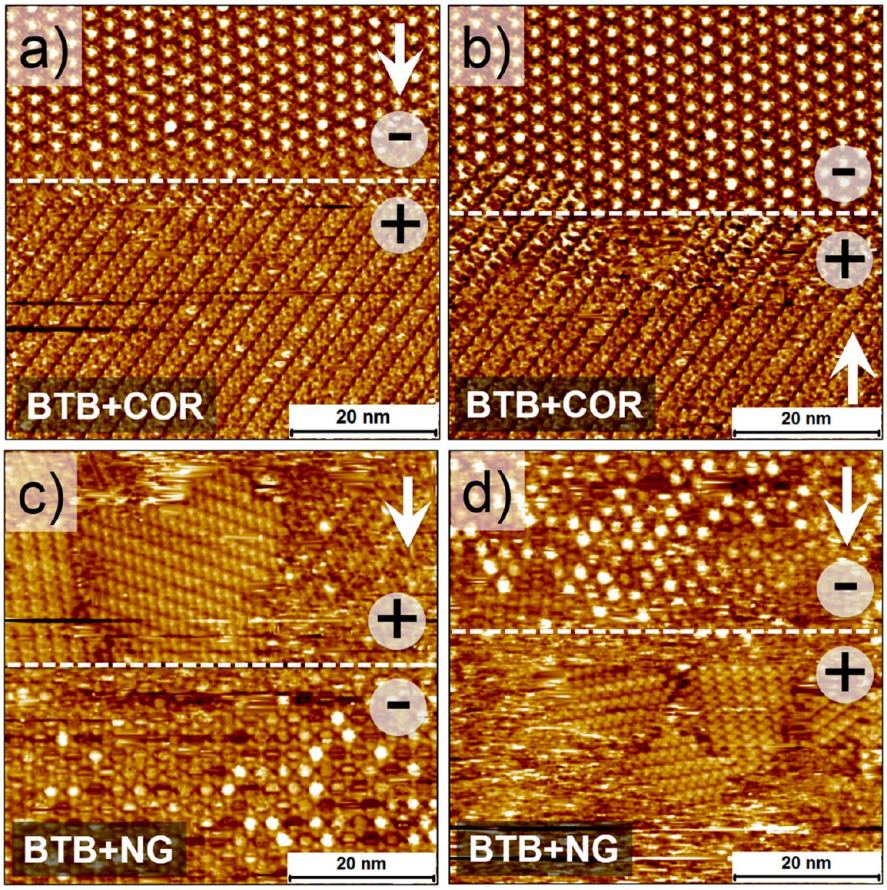

Figure 3. Voltage-induced reversible phase transition in two-component networks observed in real time. (a,b) STM images obtained by switching the polarity of sample bias for the BTB−COR system. (c,d) Similar exercise carried out for the BTB−NG system. The white dashed lines represent an approximate point at which the polarity was switched. The polarity of the sample bias is indicated on the STM images. The white arrows indicate the STM scan direction. Imaging conditions: $V_{bias} = \pm 900$ mV, $I_{set} = 100$ pA (also see Figures S6 and S7).

π-stacked structures can be significantly reduced by ultrasonication of the sample solution prior to deposition onto the HOPG surface (Figure S3). For both BTB−COR as well as BTB−NG systems, guest occupation does not change the unit cell parameters of the BTB open porous structure. The host−guest systems displayed in Figure 2 could be realized both *via* deposition of a premixed solution containing the host and the guest molecules or by deposition of a solution containing host followed by that of guests, indicating that the two-component networks are thermodynamically stable structures. In fact, compact structures obtained *via* deposition of relatively concentrated solutions also transformed into hexagonal host−guest networks upon addition of COR, thus hinting toward the thermodynamic preference of the system in the presence of guest species (Figure S5).

The host−guest systems described above allowed exciting observations when subjected to polarity-induced switching. Figure 3 shows STM images for both BTB−COR and BTB−NG systems, where the polarity of the substrate bias was switched from negative to positive and then back to negative again during an STM scan. The data indicate that when the substrate polarity is switched from negative to positive, in both cases, the host−guest network with hexagonal symmetry switches to a densely packed linear network of BTB, thus "squeezing out" the guest molecules. The reverse transition is also possible where the linear network transforms into the hexagonal network, thereby recapturing the guest molecules. As evident from the STM images, both transformations are nearly instantaneous and the networks change from one scan line to the other.

We examined the time dependence of switching for the two systems by triggering the switch a number of times and monitoring the time lapse between the appearance of the other phase. Our observations are presented in the histograms displayed in Figure 4e,f. The "delay time" plotted on the *X*-axis is defined as the time in seconds between the change in polarity and the appearance of the other phase. The histograms clearly indicate that the transition tends to occur more often at early times than at later times. A long delay between a change in the substrate polarity and the appearance of the other phase is a rather rare event, and one of such sequences of STM scans is shown in Figure 4a−d for the BTB−COR system. Even after

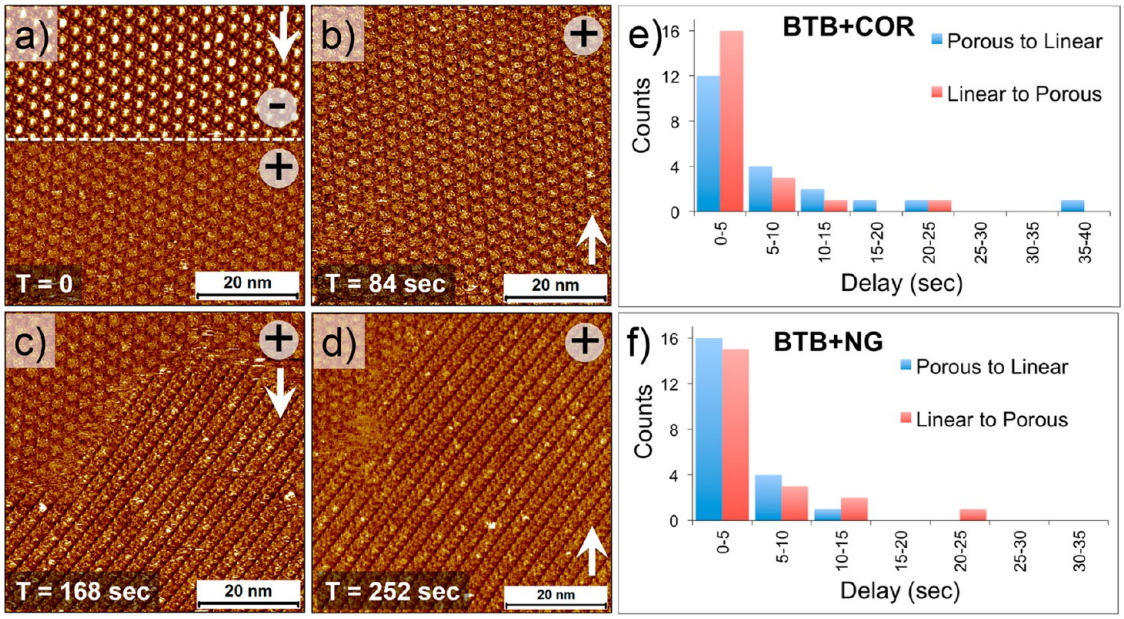

Figure 4. Time dependence of phase transition and guest release. (a–d) Consecutive STM images showing a delay in phase transition upon switching the polarity of substrate bias. It is evident from these STM images that the hexagonal structure prevalent at negative substrate bias does not change immediately upon switching the polarity of the substrate bias to positive. The linear structure appears only after a delay of *ca.* 100 s as seen in (c). (e,f) Histograms of the time dependence of switching for the two systems. The data were obtained in several experimental sessions using different tips.

the substrate polarity is switched from negative to positive, the hexagonal structure continues to be on the surface, and only after around 90 s does the linear structure start to appear. In general, the speed of the bidirectional switching for the two host–guest systems is usually as fast as that of the BTB network alone (delay time less than 10 s).[35] This observation implies that once the BTB porous network is formed, the guest molecules occupy the cavities almost instantaneously. These conclusions are in line with previous results of Eder *et al.*, where an occupation time of less than 1 s was estimated for the BTB–COR system.[38]

In switching experiments involving light, pH, ions, or heat as triggers, the surface often responds to the trigger in a rather uniform manner. However, the local nature of an STM measurement implies that the influence of the electric field and, in turn, the switching is also localized within the nanometer-scale region underneath the STM tip. While this holds true, in principle, capturing the local changes caused by the electric field directly underneath the tip is not straightforward using STM because "reading" (using an STM tip) cannot be decoupled from "writing" (also using an STM tip). Furthermore, the time scale of phase switching (few seconds) is usually faster than the typical time required to capture a relatively large-scale STM image (up to a minute). Decreasing the temperature could reduce the dynamics at the solution–solid interface, but technical problems arise due to the high melting point of the solvents (*i.e.*, OA). Thus, it is not straightforward to arrive at experimental conditions where the switching can be slowed down or the locally switched phase can be "frozen".

The intrinsic problems described above can be circumvented when working under almost solvent-free conditions in a "thin-layer" configuration. Thus, the dynamics of the bidirectional phase transition can be significantly reduced when working with host–guest monolayers where most of the solvent has evaporated. Such "semidry" monolayers can be obtained by allowing the solvent to evaporate gradually from the surface over a period of 5–6 h after drop-casting. Alternatively, contacting a tissue paper to the sample surface produces an almost-dry sample surface immediately *via* absorption of solution into the tissue. It must be noted however that, for tissue-paper-assisted drying, one has to use small volumes of sample solution since a large volume may generate strong capillary effects at the solution–solid interface that are known to affect molecular self-assembly.[40,41] In the following, we describe the outcome of switching experiments carried out on such semidry surfaces.

STM images provided in Figure 5 demonstrate the local control over switching and guest release in a semidry BTB–NG monolayer. A porous to linear transition was triggered by changing the polarity of the substrate bias from negative to positive while scanning a 50×50 nm^2 area. The phase change was followed by subsequent STM imaging of the same area over a few scans at positive substrate bias. As evident from the sequence of STM images, the area of the low-density BTB network without guest molecules (lower right) was transformed into the compact network faster than the

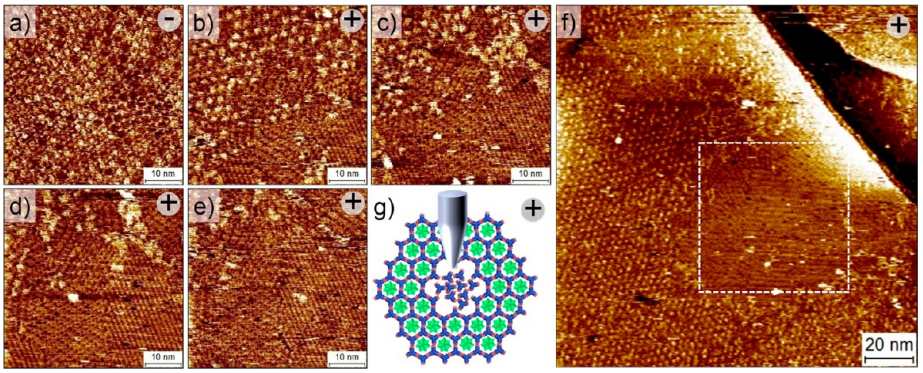

Figure 5. Demonstration of local control over switching and guest release at the 1-octanoic acid/HOPG interface. This figure shows the sequence of STM images obtained on a semidry surface for the BTB−NG system. The polarity of the sample bias is indicated on the STM images. (a) STM image of an area showing a porous BTB network containing NG guests. Not all of the cavities of the network are occupied with NG. (b−e) Sequential STM images of the same area as in (a) recorded at positive sample bias. The porous network gradually disappears, squeezing out the guest molecules, and the linear network appears. (f) Large-area STM image immediately captured after recording the small-area STM image provided in panel (e). This small area is indicated by a white square. Due to the lag in the structural transition, it is possible to capture the porous phase, which contains a small area in the middle that has been switched to the densely packed linear structure. (g) Schematic showing bias-induced local phase transition. The star-shaped green features represent the NG guest molecules. Imaging conditions: $V_{bias} = \pm 900$ mV, $I_{set} = 100$ pA.

area where the BTB cavities were occupied with NG guests. It took *ca.* 10 min for the scanned area (50 × 50 nm^2) to completely convert into the compact structure of BTB (Figure S8). This observation suggests that guest adsorption slows down the transition *via* stabilization of the host network; however, this effect is minimal (and not observed) at the solution−solid interface, possibly in view of faster dynamics. A relatively large area (145 × 145 nm^2, Figure 5f) STM image recorded after the sequence of STM images provided in Figure 5a−e showed the initially switched area (high-density BTB phase, white square) surrounded by the hexagonal BTB−NG network. This indicates that the surrounding BTB−NG network is lagging in transition despite being imaged at positive substrate bias. Further consecutive scans at positive sample bias in this larger area converted the scanned surface to the compact structure of BTB (Figure S9). When the sample bias was switched from positive to negative, the BTB−NG structures were gradually formed again, indicating that the process remained reversible for the semidried surface (Figure S10). The surface morphologies became insensitive to the change in voltage polarity upon complete removal of the solvent, indicating that the presence of a fluid medium is essential for the switching behavior.

In contrast to the local control exerted by the STM tip, one can also induce the switching globally over the entire surface by using heat as the stimulus. Gutzler *et al.* have reported a reversible transition between open and closed networks of BTB by varying the substrate temperature.[18] It must be noted here that the high-density BTB network obtained at higher temperatures is different from the compact structure discussed so far in this work. The fundamental difference in the two networks is in the alignment of BTB molecules with respect to the HOPG surface. STM images indicate that the compact structure consists of BTB molecules lying nearly flat on the HOPG surface, whereas the high-density network reported by Gutzler *et al.* comprises densely packed rows where the BTB molecules are stacked face to face and are almost standing upright. The structure is stabilized by intermolecular van der Waals and $\pi-\pi$ interactions.[18] We explored this transition in the context of host−guest system as follows.

A fast change in the temperature was achieved by *in situ* addition of a droplet of warm 1-octanoic acid (~70 °C, 10 μL) on top of a preformed BTB−NG network held at room temperature (Figure 6a). The thermal stimulus effectively triggered the phase switching of BTB from the low- to the high-density packing. This transition is gradual and can be captured in sequential STM images displayed in panels (b−e) of Figure 6. As the sample spontaneously cooled down, the reverse phase transformation was observed (Figure 6g,h). Isolated domains of NG adsorbed directly onto the surface (Figure 6f) were also detectable as long as the surface remained hot. These NG domains, however, disappeared upon gradual cooling of the sample, which is probably related to the resultant expansion of the BTB network and subsequent of formation of BTB−NG host−guest network.

It must be noted that phase-separated domains of NG were not observed for bias-induced switching in the BTB−NG system. This contrasting result can be explained on the basis of two aspects. The first relates to the nature of switching. The bias-triggered transition is effective only at the local level (around a few hundred square nanometers), and thus the NG guests released from the host network either dissolve back in the supernatant solution or are readsorbed elsewhere

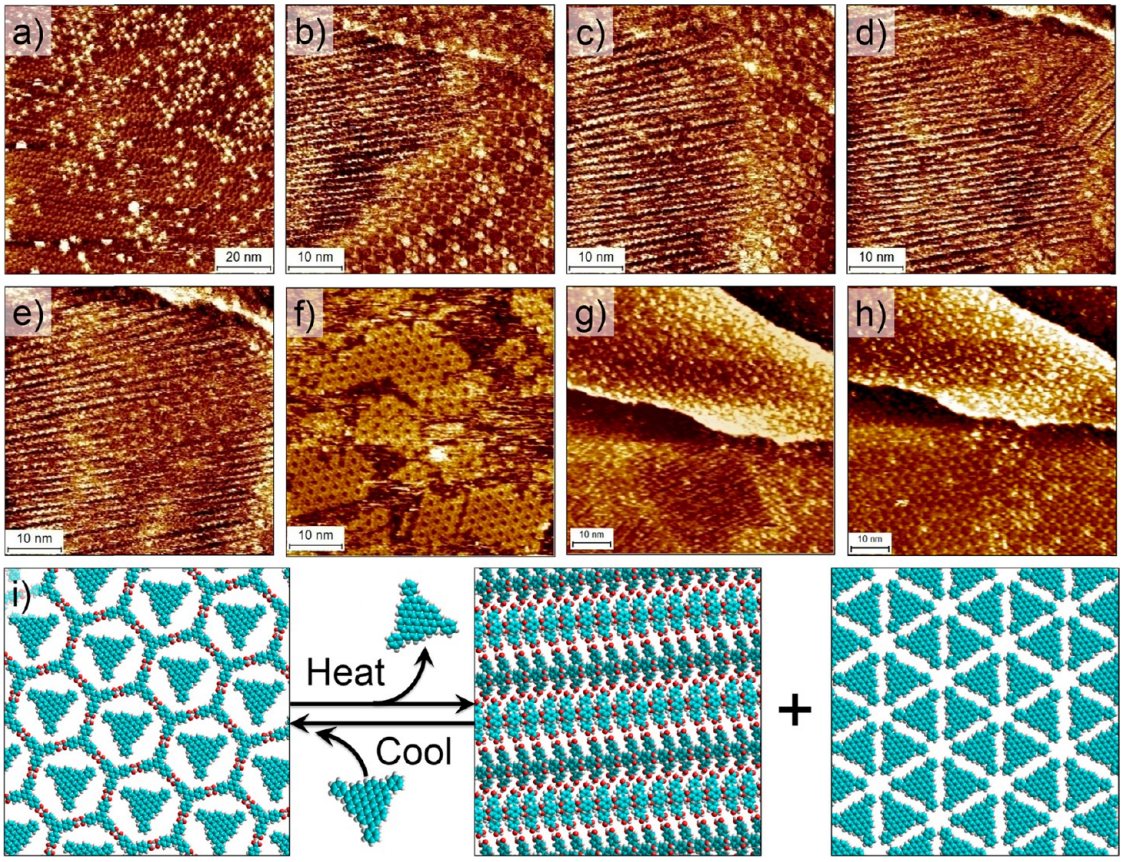

Figure 6. Heat-triggered reversible transition in the BTB–NG host–guest system. (a) STM image showing the BTB–NG network equilibrated at room temperature. (b–e) STM images of the BTB–NG monolayer obtained after addition of a droplet of warm 1-octanoic acid. The gradual transition from the hexagonal host–guest to the high-density network is clearly evident. (f) STM image showing phase-separated domains of NG adsorbed onto the HOPG surface without the host network. (g,h) STM images of the reverse phase transformation upon gradual spontaneous cooling. To avoid the impact from STM polarity, all STM images were recorded at negative substrate bias. (i) Molecular models depicting the temperature-assisted guest release and capture. Imaging conditions: V_{bias} = −900 mV, I_{set} = 100 pA.

in vacant cavities of the BTB network. In the heat-triggered transition, however, since the change happens on a global scale, the guest molecules are released from all over the surface. This increases the probability of their readsorption onto the surface. Second, the level of compression for the porous to the densely packed upright structure is much higher (80%) than that for the porous to compact transition (54%). This means that when the BTB network changes from the host–guest to the densely packed upright structure, a large area on the surface is made free for adsorption of other molecular species such as NG.

Since the thermal stimulus is expected to be somewhat homogeneous throughout the surface, switching of the whole surface is expected. To verify this hypothesis, an *ex situ* heating experiment was carried out. We heated the sample until the whole surface was dried (∼70 °C, 3 h). The patterns formed at high temperature on the dried surface did not undergo significant changes when the substrate was gradually cooled to room temperature. STM revealed that on such surfaces the densely packed row structure of BTB was the dominant phase (∼41%), and the BTB–NG, NG phases, as well as the empty surface contribute *ca.* 13, 15, and 31%, respectively, confirming the global nature of the transition in the supramolecular network (Figure S11).

The two methods of guest release and capture discussed above differ not only in terms of the nature of the trigger and the extent to which the surface is affected but also in the mechanism of switching. Cometto *et al.* have recently discussed the mechanistic aspects of the electric-field-assisted switching in BTB monolayers formed at the 1-nonanoic acid/HOPG interface.[35] They suggested that the alignment of the molecular dipole with respect to electric field upon switching of voltage polarity is responsible for the observed structural changes. They noted that this mechanism is also compatible with the formation of partially deprotonated BTB species at positive values of substrate bias that can only be assisted by water traces. The typical organic solvents used for STM experiments often contain several parts per million of water. The water molecules may act as proton acceptors at positive values of substrate bias and thus drive the transition to the compact structure. Ruben *et al.* invoked the

deprotonation hypothesis to explain temperature-induced porous to compact transition in BTB monolayers.[42] This collective information indicates that the electric field alignment of the molecular dipole may not be sufficient to explain the observed structural transitions, and partial deprotonation of the BTB species at positive substrate bias cannot be ruled out.

In the heat-assisted switching method, the transition may or may not involve deprotonation. Temperature-dependent studies carried out on BTB monolayers at the UHV–solid interface revealed transition of the open porous network to compact structure, and this transition has been explained using partial deprotonation of BTB at higher temperatures (47 °C). The compact structure, however, consists of BTB molecules lying flat on the solid surface. The densely packed upright structure observed at higher temperatures at the solution–solid interface is also observed as a stable phase at high concentrations of BTB. Gutzler *et al.* have studied the temperature-induced reversible transition between the porous and the densely packed structures of BTB from a thermodynamic point of view. Based on the estimates of the entropic cost and enthalpic gain, they suggested that the stability of the porous network at room temperature can only be explained by considering the stabilizing contributions from solvent molecules coadsorbed in the BTB cavities. At elevated temperatures, however, desorption of these weakly bound solvent molecules causes destabilization of the open porous structure, leading to the emergence of the densely packed network.[18]

We note that the adsorption of guest molecules in the BTB cavities occurs at the cost of expulsion of the dynamically coadsorbed solvent molecules. The guest molecules stabilize the host network so that it is sustained even upon removal of solvent molecules from the cavities at room temperature. Although they are not expected to interact strongly with the BTB network, both NG and COR possibly have sufficient dispersive interactions with the host network needed for its stabilization. Both the triggers employed here, namely, electric field as well as increase in temperature, bring about the structural change despite the presence of guest molecules. This indicates that the guest stabilization is not sufficient to block or slow down the transition at room temperature at the solution–solid interface. Since the guest molecules are expected to show relatively weak dependence on the polarity of the substrate (see data for NG, Figure S1 in Supporting Information), we believe that the guest release essentially occurs due to compression of the host network, which displaces the guests from the surface. It remains to be seen whether strongly interacting guests can alter the conditions over which the phase transition can be affected.

CONCLUSION AND OUTLOOK

Supramolecular nanostructures that can be externally triggered to contract or expand in a controlled manner are highly desirable in the rapidly developing field of stimuli-responsive materials. In the work described above, we have exploited dynamic reversible switching in a physisorbed self-assembled network to demonstrate controlled release and capture of guest molecules at the solution–solid interface. This unique approach exploits the changes in the individual building blocks of the network that are additive and thus produce a coherent response to either an electric or a thermal stimulus. This general method of guest release is based on the compression of the host network that results in the release of the guest molecules from the supramolecular network. The system exhibits excellent response efficiency, reversibility, and stability.

Our approach offers an alternative to the conventional systems based on chemisorbed SAMs and polymer-based systems. While polymeric systems provide a robust platform, they lack the desired high degree of internal order. Chemisorbed SAMs, while providing excellent order and robustness, need elaborate synthetic design of building blocks. The physisorbed self-assembled monolayers based on small molecules employed here are easy to fabricate and offer greater flexibility in terms of their design and function. While the novel strategy presented here bodes well for the development of alternative stimuli-responsive systems, some challenges remain. Coupling the microscopic response to the real-life macroscopic level is a major challenge, and scaling-up of the process may take this strategy a step further toward real applications. The release and capture of molecular guests in a selective fashion is also highly desirable. The integration of switchable physisorbed networks with host–guest chemistry nevertheless will confer the field of switchable systems with numerous potential applications.

EXPERIMENTAL SECTION

All STM experiments were performed at room temperature (24–25 °C) using a Nanoscope IIIa (Bruker) machine operating in constant-current mode. STM tips were prepared by mechanical cutting from a Pt/Ir wire (80%/20%, diameter 0.25 mm). 1-Octanoic acid (OA) and 1-nonanoic acid (NA) (Sigma-Aldrich, ≥99%) were used as the solvent without further purification. Prior to imaging, solid 1,3,5-tris(4-carboxyphenyl)benzene (BTB), coronene (COR), and nanographene (NG)[(1)] were dissolved in OA or NA in an appropriate amount, and a droplet of the sample solution was applied by a pipet onto a freshly cleaved surface of highly oriented pyrolytic graphite (HOPG, grade ZYB, Advanced Ceramics Inc., Cleveland, USA). The experiments were repeated in several sessions using different tips to check for reproducibility and to avoid experimental artifacts, if any. For analysis purposes, recording of a molecular image was followed by imaging the graphite lattice underneath

it under the same experimental conditions, except for lowering the bias. The images were corrected for drift *via* a scanning probe image processor software (Image Metrology ApS), using the recorded graphite images for calibration purposes, allowing a more accurate unit-cell determination. The unit-cell parameters were determined by examining at least five images, and only the average values are reported. After the determination of the unit cell from drift-corrected STM images, a molecular model of the observed monolayer was constructed using HyperChem Professional 7.5 program. First, a molecular model for a single molecule was built, and then this model was geometry-optimized in vacuum using molecular mechanics optimization (Fletcher-Reeves algorithm with rms gradient of 0.1 kcal/Å mol). Following this, a 2D crystal based on unit cell parameters obtained from calibrated STM images was built by duplicating and translating the molecules at the lattice sites. The imaging parameters are indicated in figure captions: sample bias (V_{bias}) and tunneling current (I_{set}). Histograms of the delayed time of phase switching in Figure 3 were obtained by at least 20 switching counts for each case. The data used were obtained from several experimental sessions using different tips.

Conflict of Interest: The authors declare no competing financial interest.

Acknowledgment. This work is supported by the Fund of Scientific Research—Flanders (FWO), KU Leuven (GOA 11/003), and Belgian Federal Science Policy Office (IAP-7/05). This research has also received funding from the European Research Council under the European Union's Seventh Framework Programme (FP7/2007-2013)/ERC Grant Agreement No. 340324.

Supporting Information Available: The Supporting Information is available free of charge on the ACS Publications website at DOI: 10.1021/acsnano.5b06081.

Additional details and figures (PDF)

REFERENCES AND NOTES

1. Liu, Y.; Mu, L.; Liu, B.; Kong, J. Controlled Switchable Surface. *Chem. - Eur. J.* **2005**, *11*, 2622–2631.
2. Pranzetti, A.; Preece, J. A.; Mendes, P. M. Stimuli-Responsive Surfaces in Biomedical Applications. In *Intelligent Stimuli-Responsive Materials*; John Wiley & Sons, Inc., 2013; pp 377−422.
3. Mendes, P. M. Stimuli-Responsive Surfaces for Bio-Applications. *Chem. Soc. Rev.* **2008**, *37*, 2512–2529.
4. Kudernac, T.; Ruangsupapichat, N.; Parschau, M.; Macia, B.; Katsonis, N.; Harutyunyan, S. R.; Ernst, K.-H.; Feringa, B. L. Electrically Driven Directional Motion of a Four-Wheeled Molecule on a Metal Surface. *Nature* **2011**, *479*, 208–211.
5. Pace, G.; Ferri, V.; Grave, C.; Elbing, M.; von Hänisch, C.; Zharnikov, M.; Mayor, M.; Rampi, M. A.; Samorì, P. Cooperative Light-Induced Molecular Movements of Highly Ordered Azobenzene Self-Assembled Monolayers. *Proc. Natl. Acad. Sci. U. S. A.* **2007**, *104*, 9937–9942.
6. Browne, W. R.; Feringa, B. L. Light Switching of Molecules on Surfaces. *Annu. Rev. Phys. Chem.* **2009**, *60*, 407–428.
7. Lahann, J.; Mitragotri, S.; Tran, T.-N.; Kaido, H.; Sundaram, J.; Choi, I. S.; Hoffer, S.; Somorjai, G. A.; Langer, R. A Reversibly Switching Surface. *Science* **2003**, *299*, 371–374.
8. Liu, Y.; Mu, L.; Liu, B.; Zhang, S.; Yang, P.; Kong, J. Controlled Protein Assembly on a Switchable Surface. *Chem. Commun.* **2004**, 1194–1195.
9. Ciesielski, A.; Palma, C.-A.; Bonini, M.; Samorì, P. Towards Supramolecular Engineering of Functional Nanomaterials: Pre-Programming Multi-Component 2D Self-Assembly at Solid-Liquid Interfaces. *Adv. Mater.* **2010**, *22*, 3506–3520.
10. Mali, K. S.; Adisoejoso, J.; Ghijsens, E.; De Cat, I.; De Feyter, S. Exploring the Complexity of Supramolecular Interactions for Patterning at the Liquid−Solid Interface. *Acc. Chem. Res.* **2012**, *45*, 1309–1320.
11. Ciesielski, A.; Szabelski, P. J.; Rżysko, W.; Cadeddu, A.; Cook, T. R.; Stang, P. J.; Samorì, P. Concentration-Dependent Supramolecular Engineering of Hydrogen-Bonded Nanostructures at Surfaces: Predicting Self-Assembly in 2D. *J. Am. Chem. Soc.* **2013**, *135*, 6942–6950.
12. Lei, S.; Tahara, K.; De Schryver, F. C.; Van der Auweraer, M.; Tobe, Y.; De Feyter, S. One Building Block, Two Different Supramolecular Surface-Confined Patterns: Concentration in Control at the Solid−Liquid Interface. *Angew. Chem., Int. Ed.* **2008**, *47*, 2964–2968.
13. Blunt, M.; Lin, X.; Gimenez-Lopez, M. d. C.; Schroder, M.; Champness, N. R.; Beton, P. H. Directing Two-Dimensional Molecular Crystallization using Guest Templates. *Chem. Commun.* **2008**, 2304–2306.
14. Blunt, M. O.; Russell, J. C.; Gimenez-Lopez, M. C.; Taleb, N.; Lin, X.; Schröder, M.; Champness, N. R.; Beton, P. H. Guest-induced Growth of a Surface-Based Supramolecular Bilayer. *Nat. Chem.* **2011**, *3*, 74–78.
15. Furukawa, S.; Tahara, K.; De Schryver, F. C.; Van der Auweraer, M.; Tobe, Y.; De Feyter, S. Structural Transformation of a Two-Dimensional Molecular Network in Response to Selective Guest Inclusion. *Angew. Chem., Int. Ed.* **2007**, *46*, 2831–2834.
16. Ahn, S.; Matzger, A. J. Additive Perturbed Molecular Assembly in Two-Dimensional Crystals: Differentiating Kinetic and Thermodynamic Pathways. *J. Am. Chem. Soc.* **2012**, *134*, 3208–3214.
17. Blunt, M. O.; Adisoejoso, J.; Tahara, K.; Katayama, K.; Van der Auweraer, M.; Tobe, Y.; De Feyter, S. Temperature-Induced Structural Phase Transitions in a Two-Dimensional Self-Assembled Network. *J. Am. Chem. Soc.* **2013**, *135*, 12068–12075.
18. Gutzler, R.; Sirtl, T.; Dienstmaier, J. r. F.; Mahata, K.; Heckl, W. M.; Schmittel, M.; Lackinger, M. Reversible Phase Transitions in Self-Assembled Monolayers at the Liquid−Solid Interface: Temperature-Controlled Opening and Closing of Nanopores. *J. Am. Chem. Soc.* **2010**, *132*, 5084–5090.
19. Marie, C.; Silly, F.; Tortech, L.; Müllen, K.; Fichou, D. Tuning the Packing Density of 2D Supramolecular Self-Assemblies at the Solid−Liquid Interface using Variable Temperature. *ACS Nano* **2010**, *4*, 1288–1292.
20. Bellec, A.; Arrigoni, C.; Schull, G.; Douillard, L.; Fiorini-Debuisschert, C.; Mathevet, F.; Kreher, D.; Attias, A.-J.; Charra, F. Solution-Growth Kinetics and Thermodynamics of Nanoporous Self-Assembled Molecular Monolayers. *J. Chem. Phys.* **2011**, *134*, 124702–124707.
21. Shen, Y.-T.; Deng, K.; Zhang, X.-M.; Feng, W.; Zeng, Q.-D.; Wang, C.; Gong, J. R. Switchable Ternary Nanoporous Supramolecular Network on Photo-Regulation. *Nano Lett.* **2011**, *11*, 3245–3250.
22. Tahara, K.; Inukai, K.; Adisoejoso, J.; Yamaga, H.; Balandina, T.; Blunt, M. O.; De Feyter, S.; Tobe, Y. Tailoring Surface-Confined Nanopores with Photoresponsive Groups. *Angew. Chem., Int. Ed.* **2013**, *52*, 8373–8376.
23. Bléger, D.; Ciesielski, A.; Samorì, P.; Hecht, S. Photoswitching Vertically Oriented Azobenzene Self-Assembled Monolayers at the Solid−Liquid Interface. *Chem. - Eur. J.* **2010**, *16*, 14256–14260.
24. Dri, C.; Peters, M. V.; Schwarz, J.; Hecht, S.; Grill, L. Spatial Periodicity in Molecular Switching. *Nat. Nanotechnol.* **2008**, *3*, 649–653.
25. Piot, L.; Meudtner, R. M.; El Malah, T.; Hecht, S.; Samorì, P. Modulating Large-Area Self-Assembly at the Solid−Liquid Interface by pH-Mediated Conformational Switching. *Chem. - Eur. J.* **2009**, *15*, 4788–4792.
26. Cui, K.; Mali, K. S.; Ivasenko, O.; Wu, D.; Feng, X.; Walter, M.; Müllen, K.; De Feyter, S.; Mertens, S. F. L. Squeezing, Then Stacking: From Breathing Pores to Three-Dimensional Ionic Self-Assembly under Electrochemical Control. *Angew. Chem., Int. Ed.* **2014**, *53*, 12951–12954.
27. Yoshimoto, S.; Sawaguchi, T.; Su, W.; Jiang, J.; Kobayashi, N. Superstructure Formation and Rearrangement in the Adlayer of a Rare-Earth-Metal Triple-Decker Sandwich Complex at the Electrochemical Interface. *Angew. Chem., Int. Ed.* **2007**, *46*, 1071–1074.
28. Mali, K. S.; Wu, D.; Feng, X.; Müllen, K.; Van der Auweraer, M.; De Feyter, S. Scanning Tunneling Microscopy-Induced Reversible Phase Transformation in the Two-Dimensional

Crystal of a Positively Charged Discotic Polycyclic Aromatic Hydrocarbon. *J. Am. Chem. Soc.* **2011**, *133*, 5686–5688.
29. Lei, S.-B.; Deng, K.; Yang, Y.-L.; Zeng, Q.-D.; Wang, C.; Jiang, J.-Z. Electric Driven Molecular Switching of Asymmetric Tris(phthalocyaninato) Lutetium Triple-Decker Complex at the Liquid/Solid Interface. *Nano Lett.* **2008**, *8*, 1836–1843.
30. Toader, M.; Hietschold, M. SnPc on Ag(111): A Scanning Tunneling Microscopy Study at the Submolecular Level. *J. Phys. Chem. C* **2011**, *115*, 12494–12500.
31. Zheng, Q.-N.; Liu, X.-H.; Liu, X.-R.; Chen, T.; Yan, H.-J.; Zhong, Y.-W.; Wang, D.; Wan, L.-J. Bilayer Molecular Assembly at a Solid/Liquid Interface as Triggered by a Mild Electric Field. *Angew. Chem., Int. Ed.* **2014**, *53*, 13395–13399.
32. Lee, S.-L.; Hsu, Y.-J.; Wu, H.-J.; Lin, H.-A.; Hsu, H.-F.; Chen, C.-h. Electrical Pulse Triggered Reversible Assembly of Molecular Adlayers. *Chem. Commun.* **2012**, *48*, 11748–11750.
33. Hirsch, B. E.; McDonald, K. P.; Qiao, B.; Flood, A. H.; Tait, S. L. Selective Anion-Induced Crystal Switching and Binding in Surface Monolayers Modulated by Electric Fields from Scanning Probes. *ACS Nano* **2014**, *8*, 10858–10869.
34. Ciesielski, A.; Lena, S.; Masiero, S.; Spada, G. P.; Samorì, P. Dynamers at the Solid−Liquid Interface: Controlling the Reversible Assembly/Reassembly Process between Two Highly Ordered Supramolecular Guanine Motifs. *Angew. Chem., Int. Ed.* **2010**, *49*, 1963–1966.
35. Cometto, F. P.; Kern, K.; Lingenfelder, M. Local Conformational Switching of Supramolecular Networks at the Solid/Liquid Interface. *ACS Nano* **2015**, *9*, 5544–5550.
36. Silly, F. Two-Dimensional 1,3,5-Tris(4-carboxyphenyl)-benzene Self-Assembly at the 1-Phenyloctane/Graphite Interface Revisited. *J. Phys. Chem. C* **2012**, *116*, 10029–10032.
37. Kampschulte, L.; Lackinger, M.; Maier, A.-K.; Kishore, R. S. K.; Griessl, S.; Schmittel, M.; Heckl, W. M. Solvent Induced Polymorphism in Supramolecular 1,3,5-Benzenetribenzoic Acid Monolayers. *J. Phys. Chem. B* **2006**, *110*, 10829–10836.
38. Eder, G.; Kloft, S.; Martsinovich, N.; Mahata, K.; Schmittel, M.; Heckl, W. M.; Lackinger, M. Incorporation Dynamics of Molecular Guests into Two-Dimensional Supramolecular Host Networks at the Liquid−Solid Interface. *Langmuir* **2011**, *27*, 13563–13571.
39. Lei, S.; Tahara, K.; Feng, X.; Furukawa, S.; De Schryver, F. C.; Müllen, K.; Tobe, Y.; De Feyter, S. Molecular Clusters in Two-Dimensional Surface-Confined Nanoporous Molecular Networks: Structure, Rigidity, and Dynamics. *J. Am. Chem. Soc.* **2008**, *130*, 7119–7129.
40. Lee, S.-L.; Adisoejoso, J.; Fang, Y.; Tahara, K.; Tobe, Y.; Mali, K. S.; De Feyter, S. Efficient Screening of 2D Molecular Polymorphs at the Solution-Solid Interface. *Nanoscale* **2015**, *7*, 5344–5349.
41. Lee, S.-L.; Chi, C.-Y. J.; Huang, M.-J.; Chen, C.-h.; Li, C.-W.; Pati, K.; Liu, R.-S. Shear-Induced Long-Range Uniaxial Assembly of Polyaromatic Monolayers at Molecular Resolution. *J. Am. Chem. Soc.* **2008**, *130*, 10454–10455.
42. Ruben, M.; Payer, D.; Landa, A.; Comisso, A.; Gattinoni, C.; Lin, N.; Collin, J.-P.; Sauvage, J.-P.; De Vita, A.; Kern, K. 2D Supramolecular Assemblies of Benzene-1,3,5-triyl-tribenzoic Acid: Temperature-Induced Phase Transformations and Hierarchical Organization with Macrocyclic Molecules. *J. Am. Chem. Soc.* **2006**, *128*, 15644–15651.